Inert and reacting transport

M. Cencini[1], D. Vergni[2] and A. Vulpiani[1]

August 1, 2003

[1] Dipartimento di Fisica, Università di Roma "la Sapienza" and
Center for Statistical Mechanics and Complexity INFM UdR Roma1
Piazzale Aldo Moro 5, I-00185 Roma, Italy
[2] Istituto Applicazioni del Calcolo, CNR
Viale del Policlinico 137, I-00161 Roma, Italy

Abstract

We review some aspects of passive transport in fluid flows. Two classes of problems are considered: inert substances that are simply advected by the flow, and substances that chemically (or biologically) react while are advected. Concerning the former issue, we mainly discuss the transport properties from a Lagrangian point of view. In particular, we address the problem of anomalous diffusion in the asymptotic single particle motion, and we introduce a scale dependent description of the particles pair separation evolution. This kind of description is very useful to characterize the non asymptotic properties of transport which often are the more interesting ones. For the problem of reacting transport we mainly focus on the properties of front propagation in presence of stirring. In particular, we address the dependence of the front speed on the flow characteristics, considering the case of reaction that are slow or fast with respect to the typical time scales of advection. Moreover, we discuss the role of Lagrangian chaos in the propagation properties.

1 Introduction

The transport of fields (e.g. the concentration of some species) advected by a velocity field is a problem of considerable practical and theoretical interest in many disciplines as astrophysics, geophysics, chemical engineering and disordered media [1, 2]. Though typically the advected field backreacts on the flow modifying the velocity field, often the advected field can be considered as passive, i.e. it is simply transported without affecting the velocity field. This is the case we shall consider in the following. Under this simplifying assumption, in a given velocity field the most general equation describing the evolution of the concentrations of N species, $\theta_i(\boldsymbol{x}, t)$, can be written as

$$\partial_t \theta_i + \boldsymbol{u} \cdot \boldsymbol{\nabla} \theta_i = D_i \Delta \theta_i + \frac{1}{\tau_i} f_i(\theta_1, \cdots, \theta_N) \ , \qquad (1)$$

where on the l.h.s. the second term accounts for the transport by an incompressible velocity field; on the r.h.s the first term represents molecular diffusion (D_i is the diffusion constant for the i-th specie), and the second one accounts for possible chemical or biological processes (of characteristic time scale τ_i) taking place among the different substances.

In this contribution we shall consider separately the problem of inert transport when the substance is simply advected by the flow (i.e. $f_i(\theta_1, \cdots, \theta_N) = 0$), and that of reacting transport when reaction processes occur while the fields are advected.

As far as inert transport is concerned, one usually considers a unique field θ that evolves according to the advection-diffusion equation

$$\partial_t \theta + \boldsymbol{u} \cdot \boldsymbol{\nabla} \theta = D \Delta \theta \,, \tag{2}$$

being D the molecular diffusivity; eventually a source term, which represents the injection of scalar fluctuations, may be added in the r.h.s.. Given the field $\mathbf{u}$ the main goal is to understand the dynamical and statistical properties of the field θ. Remarkably, in the last few years, many progresses have been registered in this direction and we now have a satisfactory understanding of the statistics of passive fields. A crucial role in these achievements has been played by the understanding of the statistical properties of the motion of advected passive particles. The interested reader may consult the recent review [3] where an exhaustive discussion on passive fields in turbulent flows can be found.

The understanding of particles motion is important because Eq. (2) is nothing but the Fokker-Planck equation of the stochastic process describing the motion of test particles:

$$\dot{\boldsymbol{x}}(t) = \boldsymbol{u}(\boldsymbol{x}(t), t) + \sqrt{2D} \boldsymbol{\xi}(t) \tag{3}$$

where $\mathbf{u}(\boldsymbol{x}(t), t)$ is the Eulerian velocity field at the particle position $\mathbf{x}(t)$, and ξ is a Gaussian white noise with zero mean and $\langle \xi_i(t) \xi_j(t') \rangle = \delta_{ij} \delta(t - t')$.

After the seminal works of Arnold and Aref it is now well recognized that particle motion can be highly nontrivial even in simple laminar velocity fields due to the so-called Lagrangian chaos [4]. Therefore already the single particle motion presents very interesting features. For instance, the dispersion properties are greatly enhanced by the combined effects of the molecular diffusivity and the advection by the velocity fields [1, 4]. Indeed at very large times and scales (with respect to the typical time and length scales of $\boldsymbol{u}$), the test particle undergoes a Brownian process with an enhanced diffusion coefficient [5], i.e. $\langle (x_i(t) - x_i(0))^2 \rangle \simeq 2 \; D^E_{ii} \; t$ where eddy diffusion coefficient $D^E_{ii} > D$ contains the effect of the velocity field. In terms of the field θ this means that the coarse-grained concentration $\langle \theta \rangle$ (where the average is over a volume of linear dimension larger than the typical velocity length scale) obeys a standard diffusion Fick equation:

$$\partial_t \langle \theta \rangle = D^E_{ij} \partial^2_{x_i x_j} \langle \theta \rangle \qquad i, j = 1, \ldots, d \,, \tag{4}$$

where d is the space dimension. To compute D^E given the velocity field there are now well established mathematical techniques (see e.g. [5, 6]).

Moreover, it is also well known that under certain conditions anomalous diffusion takes place, i.e. $\langle (x(t) - x(0))^2 \rangle \sim t^{2\nu}$ with $\nu \neq 1/2$ [2]. Here we shall discuss in details the necessary conditions to observe anomalous diffusion. In particular, we consider the case of incompressible velocity fields where either standard diffusion ($\nu = 1/2$) or superdiffusion ($\nu > 1/2$) may appear [5].

Though interesting and relevant to many problems, the single particles motion is essentially determined by the large scale properties of the velocity field, which often hide much more interesting phenomena taking place at small scales. Moreover, the standard or anomalous diffusive properties are asymptotic features that in realistic situations may not be attained. In this sense it can be more interesting to study the relative motion of two particles. This is indeed characterized by a variety of behaviors in dependence on the statistics of the velocity field at different length scales. For instance, at very small scales (where the velocity field is smooth) particles separate exponentially, i.e. $\langle \ln |\boldsymbol{x}_2(t) - \boldsymbol{x}_1(t)| \rangle \sim \lambda t$, being λ the Lyapunov exponent. On the other hand, in the inertial range of fully developed turbulent flows particle separates as $\langle |\boldsymbol{x}_2(t) - \boldsymbol{x}_1(t)|^2 \rangle \sim t^3$, i.e. the Richardson dispersion law holds, in spite of the diffusive single particle behavior at large scales. Since, as shown in the above example, the relative dispersion properties depend on the behavior of the velocity field at different scales, we introduce a scale dependent description of particle pairs separation in term of the Finite Size Lyapunov Exponent [7]. This kind of description is also very useful to account for the non asymptotic properties of dispersion and, e.g., to describe transport in finite systems where finite size effects are present.

The problem of reacting transport is much more difficult, because the presence of the production term $f_i(\theta_1, \dots, \theta_N)$ in the transport equation (1) makes it to be non linear and new phenomena appear. Here we consider the simplest non trivial case of Eq. (1), i.e.: a unique scalar field $\theta(\mathbf{x}, t)$ evolving according to the advection-diffusion-reaction equation

$$\partial_t \theta + \boldsymbol{u} \cdot \boldsymbol{\nabla} \theta = D \Delta \theta + \frac{1}{\tau} f(\theta) \,. \tag{5}$$

Where θ represents the fractional concentration of the reacting substance with the following glossary: $\theta = 0$ indicates fresh material which still has to react, $0 < \theta < 1$ means coexistence of fresh material and products, and $\theta = 1$ is when the reaction is over [8]; equivalently one may think of θ as the concentration of a biological organism which is transported by the flow and grows according to the dynamics $f(\theta)$ [9]. Although very generic form can be considered for $f(\theta)$ (see [8, 9]) here we mainly discuss the case of $f(\theta)$ which are convex functions ($f''(\theta) < 0$) with $f(0) = f(1) = 0$ and $f'(0) = 1$. A typical example is $f(\theta) = \theta(1-\theta)$. This class of production terms belong to the so-called Fisher-Kolmogorov-Petrovsky-Piscounoff (FKPP) type [10, 11]. With this choice $\theta = 0, 1$ are the unstable and stable steady states of the dynamics, respectively. Once at the initial time a small portion of the system is such that $\theta \neq 0$ the reaction starts and a front connecting the unstable and stable states propagates.

In absence of stirring, $\boldsymbol{u} = 0$, it is known that Eq. (5), for FKPP nonlinearity, generates a front propagating, e.g., from left to right with asymptotic speed $v_0 = 2\sqrt{D/\tau}$, and the thickness of the reaction region is $\xi = 8\sqrt{D\tau}$ [10, 11]. It is worth recalling that the problem of front propagation has been extensively studied in many different fields [12, 13] such as chemical reaction fronts [8], flames propagation in gases [9] and population dynamics of biological communities [12, 13]. In many of this systems the reaction takes place in moving media, i.e. fluids, so that it is important to understand how the presence of a flow modifies the propagation properties.

As a generic feature, in presence of a non-zero velocity field the front will propagate with an average speed $v_{\rm f}$ greater than v_0 [14, 15, 16]. However, if $f(\theta)$ is not convex there are also circumstances in which the flow may stop ("quench") the reaction [17].

The front velocity $v_{\rm f}$ is the result of the interplay among the flow characteristics (i.e. intensity U and length-scale L), the diffusivity D and the production time scale τ. Here our major concern will be to discuss the dependence of $v_{\rm f}$ on such quantities. For instance, introducing the Damköhler number $Da = L/(U\tau)$ (the ratio of advective to reactive time scales) and the Péclet number $Pe = UL/D$ (the ratio of diffusive to advective time scales), one can seek for an expression of the front speed as an adimensional function $v_{\rm f}/v_0 = \phi(Da, Pe) \geq 1$. In particular, we study the case of cellular flows. We will see that a crucial role in determining $\phi(Da, Pe)$ is played by the renormalization of the diffusion coefficient and chemical time scale induced by the advection [14]. Moreover, we consider an important limit case, i.e., the so called geometrical optics limit, which is realized for $(D, \tau) \to 0$ maintaining D/τ constant [18]. In this limit one has a non zero bare front speed, v_0, while the front thickness ξ goes to zero, i.e., the front is sharp. Physically speaking, this limit corresponds to situations in which ξ is very small compared with the other length scales of the problem. Also in this case we provide a simple prediction for the front speed, which turns out to be expressible as an adimensional function $v_{\rm f}/v_0 = \psi(U/v_0)$.

Other interesting questions concern the modification of the front geometry as a consequence of advection. In particular, one may ask if the presence of Lagrangian chaos has a role in front dynamics. We shall briefly discuss this problem in the framework of the geometrical optics limit.

The material is organized as follows. In Section 2 we discuss single particle and two-particles motion in laminar and turbulent flows. Emphasis is put on the conditions for anomalous diffusion and on the non-asymptotic properties of particles pairs separation. Section 3 is devoted to the study of front propagation in fluid flows. After a brief discussion on some general results which do not depend on the specific properties of the velocity field we shall analyze in details the case of cellular flows in different regimes.

2 Transport of inert substances

As stated in the introduction the dynamical and statistical properties of advected passive fields are tightly related to those of Lagrangian particles. Therefore, from the study of particle motion one can predict many aspects of the dynamics of advected scalar fields.

Investigating the diffusive properties of single particle motion allows to predict the characteristics of the macroscopic motion of concentration fields (cfr. Eq. (4)). In this framework it is important to identify the conditions which may lead to anomalous diffusion that brings as a consequence the failure of the Fickian description of transport. Under these circumstances Eq. (4) does not hold anymore.

On the other hand the small scale features of the scalar field can be understood studying the relative motion of test particles, as the following discussion will clarify. Consider for instance the transport equation for θ

$$\partial_t \theta + \mathbf{u} \cdot \nabla \theta = D \Delta \theta + \Phi \,, \tag{6}$$

where we added an external source of tracer fluctuations, Φ, which acts at a given length scale L_Φ. The link with particle trajectories is evident by solving (6) with the method of characteristics:

$$\begin{array}{rcl} \theta(\mathbf{x},t) & = & \int_{-\infty}^{t} ds\, \Phi(\mathbf{x}(s;t),s) \\ \dot{\mathbf{x}}(s;t) & = & \mathbf{u}(\mathbf{x}(s;t),s) + \sqrt{2D}\, \boldsymbol{\xi}(s)\,, \qquad \mathbf{x}(t;t) = \mathbf{x}\,; \end{array} \tag{7}$$

the second equation is nothing but Eq. (3) where we explicitly fixed the final position to be $\boldsymbol{x}$. By using (7) one can then connect the statistics of particle trajectories to the correlation functions of the scalar field. For instance, let us consider the simultaneous two-point correlations

$$\langle \theta(\mathbf{x}_1,t)\theta(\mathbf{x}_2,t)\rangle = \int_{-\infty}^{t} ds_1 \int_{-\infty}^{t} ds_2\, \langle \Phi(\mathbf{x}_1(s_1;t),s_1)\Phi(\mathbf{x}_2(s_2;t),s_2)\rangle\,, \tag{8}$$

with $\mathbf{x}_1(t;t) = \mathbf{x}_1$ and $\mathbf{x}_2(t;t) = \mathbf{x}_2$. With a convenient choice of the correlation function of the forcing, e.g. $\langle \Phi(\mathbf{x}_1,t_1)\Phi(\mathbf{x}_2,t_2)\rangle = \chi(|\mathbf{x}_1 - \mathbf{x}_2|)\delta(t_1 - t_2)$, and exploiting space homogeneity, Eq. (8) can be further simplified to the form

$$C_2(R) = \langle \theta(\boldsymbol{x},t)\theta(\boldsymbol{x}+\boldsymbol{R},t)\rangle = \int_{-\infty}^{t} ds \int d\boldsymbol{r}\, \chi(\boldsymbol{r})\, p(\mathbf{r},s|\boldsymbol{R},t)\,. \tag{9}$$

where $p(\boldsymbol{r},s|\boldsymbol{R},t)$ is the probability density function for a pair to be at a separation $\mathbf{r}$ at time s, under the condition to have a separation $\boldsymbol{R}$ at time t. It is now clear that the knowledge of $p(\boldsymbol{r},s|\boldsymbol{R},t)$ allows to predict the behavior of C_2 and so of the scalar spectrum.

Moreover, assuming that $\chi(r)$ drops to zero for $r > L_f$ and $\chi(0) = \chi_0$, (9) may be approximated as $C_2(R) \approx \chi_0 T(R;L_f)$, where $T(R;L_f)$ is the average time the particles took to reach a separation $O(L_f)$ starting from a separation R (while going backward in time). This calls also for studying relative dispersion in terms of the time $T(R_1;R_2)$ needed to reach a separation R_2 being started from R_1. As we shall see, this is at the core of our approach to relative dispersion.

Similar reasonings can be extended to correlations functions involving more than two points. This leads to consider the relative motion of more than two particles, which may be highly non trivial [19]. A detailed discussion of this aspects is beyond our aims, therefore we limit our discussion to single and two particles properties. The interested reader may consult [3] for a discussion on the more than two particles aspects and their consequences on the scalar field properties.

2.1 Standard and anomalous diffusion

Let us discuss now the problem of absolute dispersion of a particle by recalling some well established results on the relation between diffusion phenomena and the velocity correlation function. From Eq. (3) it is easy to obtain the following relation [20]:

$$\langle (x_i(t) - x_i(0))^2 \rangle = \int_0^t dt_1 \int_0^t dt_2 \langle v_i(\boldsymbol{x}(t_1))\, v_i(\boldsymbol{x}(t_2))\rangle \simeq 2\, t \int_0^t d\tau\, C_{ii}(\tau)\,, \tag{10}$$

where

$$C_{ij}(\tau) = \langle\, v_i(\boldsymbol{x}(\tau))\; v_j(\boldsymbol{x}(0))\,\rangle \tag{11}$$

is the correlation function of the Lagrangian velocity, $\boldsymbol{v} = \dot{\boldsymbol{x}}$.

From Eq. (10) it is not difficult to understand that anomalous diffusion occurs when one, or both, of the following conditions are violated

i) finite variance of the velocity: $\langle v^2 \rangle < \infty$

ii) fast enough decay of the auto-correlation function of Lagrangian velocities: $\int_0^t d\tau\; C_{ii}(\tau) < \infty$.

If both $\langle v^2 \rangle < \infty$ and $\int_0^t d\tau\; C_{ii}(\tau) < \infty$ then one has standard diffusion and the effective diffusion coefficients are

$$D^E_{ii} = \lim_{t\to\infty} \frac{1}{2\,t} \langle (x_i(t) - x_i(0))^2 \rangle = \int_0^\infty d\tau\; C_{ii}(\tau)\,. \tag{12}$$

Let us now examine two examples in which the above conditions are violated and anomalous diffusion takes place. It is worth remarking that here we use the term anomalous diffusion to indicate a non standard diffusion in the asymptotic regime. Sometimes in the literature the term anomalous is used also for long (but non asymptotic) transient behaviors.

Violation of *i)* can be obtained in the so-called Lévy flight model [21]. The simplest instance is the discrete (in time) one dimensional case, where the particle position $x(t+1)$ at the time $t+1$ is obtained from $x(t)$ as follows:

$$x(t+1) = x(t) + U(t), \tag{13}$$

and $U(t)$'s are independent variables identically distributed according to a α–Lévy–stable distribution, $P_\alpha(U)$, i.e.:

$$\int dU e^{ikU} P_\alpha(U) \propto e^{-c|k|^\alpha} \quad \text{and} \quad P_\alpha(U) \sim U^{-(1+\alpha)} \quad \text{for} \quad |\,U\,| \gg 1 \tag{14}$$

with $0 < \alpha \leq 2$. An easy computation gives $\langle x(t)^q \rangle = C_q\; t^{q/\alpha}$ if $q < \alpha$, and $\langle x(t)^q \rangle = \infty$ if $q \geq \alpha$. Though $\langle x^2 \rangle = \infty$ for any $\alpha < 2$, one can consider the Lévy flight as a sort of anomalous diffusion in the sense that $x_{\text{typical}} \sim t^{1/\alpha} \gg t^{1/2}$. However, in spite of the relevance of the α–Lévy–stable distribution in probability theory, the Lévy flight model, in our opinion, has a rather weak importance for physical systems. This is due to the very unrealistic property of infinite variance.

Physically more interesting is the Lévy walk model [22], that is still described by (13) but now $U(t)$ is a random variable with finite variance but nontrivial correlations, so that *ii)* is violated. Let us assume that $U(t)$ can assume the values $\pm u_0$ and it maintains its value for a duration T which is a random variable with probability density $\psi(T)$. The origin of the possible anomaly is transferred to the correlation function of the Lagrangian velocity: the idea is that one has to generate a correlation such that $C_{ii}(\tau) \sim \tau^{-\beta}$ with $\beta < 1$. By taking $\psi(T) \sim T^{-(\alpha+1)}$ one has standard diffusion if $\alpha > 2$ while for $\alpha < 2$ one has anomalous (super) diffusion :

$$\langle x(t)^2 \rangle \sim t^{2\nu} \qquad \nu = \begin{cases} 1/2 & \alpha > 2 \\ (3-\alpha)/2 & 1 < \alpha < 2 \\ 1 & \alpha < 1. \end{cases} \tag{15}$$

Besides the above simplified models, more interesting is the understanding of the anomalous diffusion in incompressible velocity fields or deterministic maps. In this direction Avellaneda, Majda and Vergassola [23, 24] obtained a very important and general result about the asymptotic diffusion in an incompressible velocity field $\boldsymbol{u}(\boldsymbol{x})$. If the molecular diffusivity D is non zero and the infrared contribution to the velocity field are weak enough, namely

$$\int d\boldsymbol{k} \, \frac{\langle |\, \hat{\boldsymbol{u}}(\boldsymbol{k}) \,|^2 \rangle}{k^2} < \infty \tag{16}$$

then one has standard diffusion, i.e. the effective diffusion coefficients D^E_{ii}'s in (12) are finite. The average $\langle \cdot \rangle$ indicates the time average and $\hat{\boldsymbol{u}}$ is the Fourier transform of the velocity. There exist then two possible origins for the superdiffusion

a) $D > 0$ and, in order to violate the (16), the velocity field with very long spatial correlation;

b) $D = 0$ and strong correlation between $\boldsymbol{v}(\boldsymbol{x}(t))$ and $\boldsymbol{v}(\boldsymbol{x}(t+\tau))$ at large τ.

One of the few nontrivial systems for which the presence of anomalous diffusion can be proved in a rigorous is the $2d$ random shear flow $\mathbf{u} = (u(y)\ ,\ 0)$ where $u(y)$ is a random function [6] such that

$$u(y) = \int_{-\infty}^{\infty} dk \; e^{iky} \; \hat{u}(k) \qquad \langle \hat{u}(k) \; \hat{u}(k') \rangle = S(k) \; \delta(k - k'), \tag{17}$$

$S(k)$ is the power spectrum and the average $\langle \cdot \rangle$ is taken over the field realizations. Matheron and De Marsily [25] showed that the anomalous diffusion in the x-direction occurs if $\int dk \; S(k) k^{-2} = \infty$. On the contrary, if this integral is finite one has standard diffusion and with an effective diffusivity $D^E_{11} \gg D$. Consider now a spectrum such as $S(k) \sim k^\zeta$ for $k \mapsto 0$, it is then easy to realize that if $\zeta > 1$ standard diffusion takes place, while, if $-1 \leq \zeta \leq 1$ one has a superdiffusion [5]

$$\langle \,|\, x(t) - x(0) \,|^2 \,\rangle \sim t^{2\nu} \qquad \nu = \frac{3 - \zeta}{4} \geq \frac{1}{2}. \tag{18}$$

The condition for the anomalous diffusion $\int dk \; S(k) \; k^{-2} = \infty$ has the following physical interpretation. Dimensionally $\int dk \; S(k) \; k^{-2} \sim \langle u^2 \rangle \; L^2$ where L is the typical length of the function $u(y)$, i.e. the typical distance between two sequent zeros of $u(y)$. If $\langle u^2 \rangle < \infty$ and $\int dk \; S(k) \; k^{-2} < \infty$ the diffusion process is basically similar to that one characterized by a velocity field given by a sequence of strips of size L and velocity $\pm\sqrt{\langle u^2 \rangle}$, i.e. the transversal Taylor diffusion in channels [26]. The origin of the anomalous diffusion in this case is due to the fact that a test particle travels in a given direction for a very long time before changing direction and so on.

2.2 A remark about the meaning of *anomalous*

Let us now discuss in more general terms the anomalous diffusion problem considering the behavior of the displacement moments of arbitrary order. Two different possibilities can be distinguished [27]: *weak* anomalous diffusion where a unique exponent is relevant

$$\langle| x(t) - x(0) |^q\rangle \sim t^{q\nu} \quad \forall q > 0 \text{ and } \nu > \frac{1}{2}; \tag{19}$$

strong anomalous diffusion when

$$\langle| x(t) - x(0) |^q\rangle \sim t^{q\,\nu(q)} \quad \nu(q) \neq const \quad \nu(2) > \frac{1}{2} \tag{20}$$

and $\nu(q)$ is a nondecreasing function of q.

In terms of the probability $P(\Delta x, t)$ of observing a displacement $\Delta x = x(t) - x(0)$ at time t, weak anomalous diffusion amounts to the scaling property:

$$P(\Delta x, t) = t^{-\nu} F(\Delta x\, t^{-\nu}) \tag{21}$$

where the function F is not necessarily the Gaussian one. On the other hand strong anomalous diffusion is not compatible with the scaling (21).

In the case of weak anomalous diffusion, it is natural to conjecture

$$F(z) \propto e^{-c|z|^\alpha}, \tag{22}$$

where in general α is not determined by ν. However, an argument á la Flory due to Fisher [28] suggests that

$$P(\Delta x, t) \sim t^{-\nu} \exp\left[-c\left(\frac{|\Delta x|}{t^\nu}\right)^{\frac{1}{1-\nu}}\right], \tag{23}$$

i.e., $\alpha = \frac{1}{1-\nu}$. Remarkably the random shear flow examined in the previous section is in agreement with the Fisher's prediction, indeed Bouchaud at al. [29] have shown that for $\zeta = 0$ i.e. $\nu = 3/4$ one has $F(a) \sim e^{-c|a|^4}$ for $| a | \gg 1$. While for the properties of dispersion the detailed functional dependence of $P(x,t)$ is not very important, it has an important role in determining the propagation properties in reactive systems [30].

2.3 *Strong* anomalous diffusion in chaotic flows

If (16) holds then anomalous diffusion may appear only for $D = 0$ and very strong Lagrangian velocity correlations. The latter condition can be realized, e.g., in time periodic velocity fields in which the Lagrangian phase space has a complicated self-similar structure of island and cantori [31]. In such a case superdiffusion is essentially due to the almost trapping of the ballistic trajectories for arbitrarily long time, close to the cantori which are organized in complicated self-similar structures.

In this framework an interesting example is the Lagrangian motion in velocity field given by a simple model which mimics the Rayleigh–Bénard convection [32], and is described by the stream function:

$$\psi(x, y, t) = \psi_0 \sin\left[\frac{2\pi}{L}(x + B\sin\omega t)\right] \sin\left[\frac{2\pi}{L}y\right], \tag{24}$$

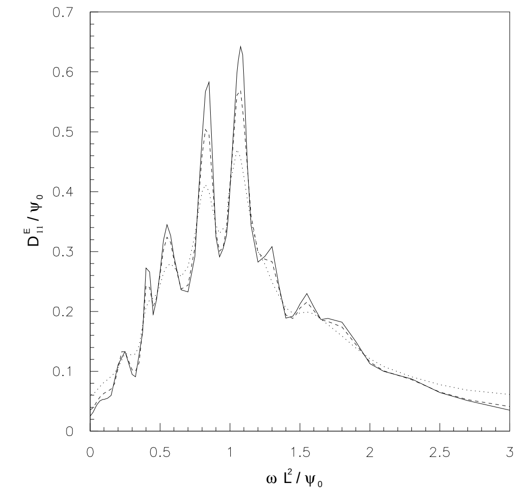

Figure 1: The turbulent diffusivity D_{11}^E/ψ_0 *vs* the frequency $\omega L^2/\psi_0$ for different values of the molecular diffusivity D/ψ_0. $D/\psi_0 = 3\times 10^{-3}$ (dotted curve); $D/\psi_0 = 1\times 10^{-3}$(broken curve); $D/\psi_0 = 5\times 10^{-4}$ (full curve).

where the velocity is given by $\boldsymbol{u} = (\partial_y\psi, -\partial_x\psi)$, $\psi_0 = UL/2\pi$ (being L the periodicity of the cell, here we use $L = 2\pi$) and U the velocity intensity. The even oscillatory instability is accounted for by the term $B\sin\omega t$, representing the lateral oscillation of the rolls [32]. At fixed B, the control parameter for particle diffusion is $\epsilon \equiv \omega L^2/\psi_0$, i.e., the ratio between the lateral roll oscillation frequency (ω) and the characteristic circulation frequency (ψ_0/L^2) inside the cell. Different regimes take place for different values of ϵ. For instance, at $\epsilon \sim 1$ the synchronization between the circulation in the cells and their global oscillation is a very efficient way of jumping from cell to cell. This mechanism, similar to stochastic resonance, makes the effective diffusivity as a function of the frequency ω very structured [27] (see Fig. 1). Moreover, in the limit of vanishing molecular diffusivity, anomalous superdiffusion takes place in a narrow window of ω values around the peaks, i.e.

$$\langle (x(t) - x(0))^2\rangle \propto t^{2\nu(2)} \qquad \text{with} \qquad \nu(2) > 1/2 \quad . \tag{25}$$

as reported in Fig. 2 (left). The presence of genuine anomalous diffusion is confirmed by the fact that effective diffusivity diverges as $D_{11}^E \sim D^{-\beta}$ with $\beta > 0$ (see Fig. 2 (right)), as suggested in [5].

The remarkable property of the flow (24) is that the moments of the particle displacement display a strong anomalous behavior (20), indeed Fig. 3 (left) shows that $q\,\nu(q)$'s is a non-trivial function of q. In particular, the curve $q\,\nu(q)$ vs q, as a whole, displays a nonlinear behavior, the first clue of anomalous diffusion in the strong sense. A closer inspection shows that two linear regions are present: the first one behaves up to $q \sim 2$, the second elsewhere. The two linear regions are associated to two different mechanisms in the diffusion process. For small q's, i.e. for the core of the probability distribution function $F(\Delta x, t)$, only one exponent ($\nu_1 \equiv \nu(q) \simeq 0.65$ for $q < 2$) fully characterizes the diffusion process. This means that the typical, i.e. non rare, events obey a (weak) anomalous diffusion process, roughly speaking, one can say that at scale l the characteristic time $\tau(l)$ behaves like $\tau(l) \sim l^{1/\nu_1}$. On the other hand, the behavior $q\,\nu(q) \simeq q - 1.04$ suggests that the large deviations are essentially associated to ballistic transport, $\tau(l) \sim l$, basically due to the mechanism of synchronization between the circulation in the cells and their global oscillation.

The character of strong anomalous diffusion, already evident from the non-trivial dependence of $\nu(q)$ on q, is also highlighted by the normalized probability densities $P(\Delta x, t)$ at different times that do not collapse onto a unique curve (see Fig. 3 (right)) suggesting that the scaling property (21) does not hold.

The above results for the anomalous diffusion in $2d$ time periodic incompressible flow may be encountered also in other systems. For instance, they had been observed also for the standard map [33]:

$$\begin{cases} J_{t+1} = J_t + K\sin(\theta_t) \\ \theta_{t+1} = \theta_t + J_{t+1} \qquad \mod 2\pi. \end{cases} \tag{26}$$

Where for specific values of K one has the coexistence of many accelerator modes, i.e. ballistic trajectories, and one observes:

$$\langle [J_t - J_0]^2 \rangle \sim t^{2\nu(2)} \qquad t \gg 1 \quad \text{with} \quad \nu(2) \neq 1/2\,, \tag{27}$$

i.e. anomalous diffusion in the action variable. The sticking of the chaotic orbits to stable islands leads to the appearance of blocks of long range correlation in the sequences of the J_t variable which are responsible for its anomalous behavior [34].

The results of this section, as well as those in [35], suggest that the phenomenon of anomalous diffusion in smooth chaotic dynamics with very long time correlation is possible but rare. For specific values of the parameters, i.e. K or ω, one can have $\nu(2) > 1/2$ but a small change typically restores the standard scenario $\nu(2) = 1/2$.

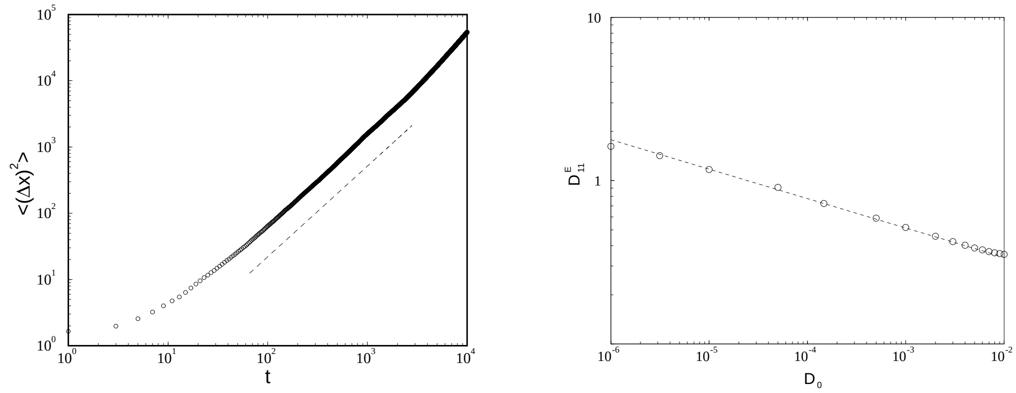

Figure 2: (left) Mean-squared displacement *vs* the time for the flow (24) with $D = 0$, and $\omega = 1.1$. Lengths and times are shown in units of L and L^2/ψ_0, respectively. The best-fit (dashed) line corresponds to $2\nu(2) = 1.3$. (right) The diffusion coefficient D_{11}^E as a function of D for the frequency of the roll oscillation $\omega = 1.1$. The diffusivities are reported in units of ψ_0. The best-fit (dashed) line has the slope $-\beta = -0.18$.

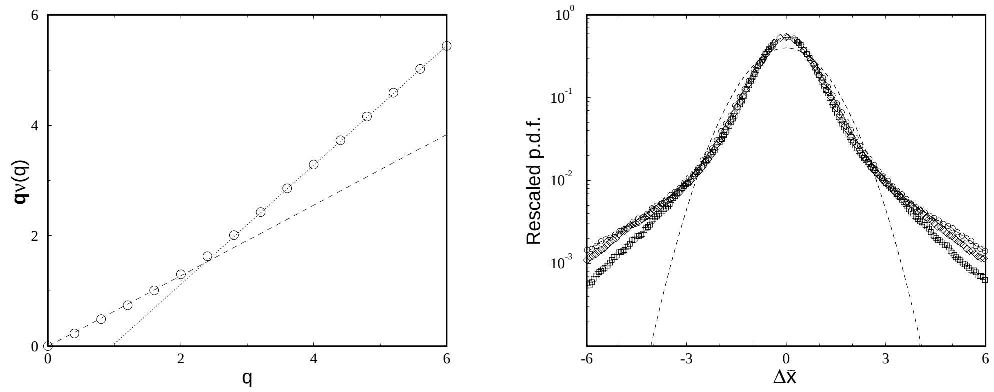

Figure 3: (left) The measured scaling exponents $q\,\nu(q)$'s (joined by dot-dashed straight lines) of the moments of the displacement Δx, as a function of the order q. The dashed line corresponds to $0.65\ q$ while the dotted line corresponds to $q - 1.04$. (right) The normalized probability distribution function $P(\Delta x(t)/\tilde{\sigma})$ vs $\Delta\tilde{x} \equiv \Delta x/\tilde{\sigma}$ (being $\tilde{\sigma} = \exp\langle \ln \mid \Delta x(t) \mid \rangle$) for the three times $t_1 = 500$ (circles), $t_2 = 2t_1$ (diamond) and $t_3 = 2t_2$ (squares). The dashed line represents the Gaussian function.

2.4 Relative dispersion

So far we limited our discussion to the single particle properties, i.e. absolute dispersion. Let us now consider the relative dispersion of two particles, $\boldsymbol{R}(t) = \boldsymbol{x}_2(t) - \boldsymbol{x}_1(t)$, that is linked to the velocity field properties at different length-scales, indeed

$$\frac{d\boldsymbol{R}}{dt} = \delta_R \boldsymbol{v} = \boldsymbol{v}(\boldsymbol{x}_1(t) + \boldsymbol{R}(t), t) - \boldsymbol{v}(\boldsymbol{x}_1(t), t)\,. \tag{28}$$

Since in incompressible flows the separation $\boldsymbol{R}$ typically grows in time [36], from the evolution of the relative separation we can, in principle, extract the contributions of the velocity components at different scales. In this sense relative dispersion studies provide a much richer information than the absolute ones. Of course, if the spatial extension of the system is infinite in the asymptotic time and space limit the two descriptions are equivalent and should give the same information. However, for finite systems, and more in general when the flow is characterized by different regimes as a function of the scale separation the relative dispersion is more interesting than the absolute one, which is simply dominated by the sweeping induced by large scale flow.

Here we consider both laminar and turbulent flows. A typical situation of interest, e.g. in geophysics, is when the the Eulerian velocity field is characterized by two length-scales: the (small) scale l_η below which the velocity is smooth (i.e. $\delta_R v \sim R$ if $R \ll l_\eta$), and a (large) scale L_0 representing the size of the largest structures present in the flow, above which the velocity differences are essentially uncorrelated. In most non turbulent flows $l_\eta \sim L_0$, while when the flow is turbulent (i.e. the Reynolds number is very high) the two scales are well separated. The interval of scales $l_\eta \ll r \ll L_0$ defines then the so-called inertial range where velocity differences display a non-smooth behavior: $\delta_r v \sim r^h$ with $h < 1$, e.g. $h = 1/3$ in Kolmogorov 1941 turbulence [37]. Moreover, one can also consider the presence of boundaries in the system, e.g. of size L_B.

The presence of these regimes manifests in different behaviors of the particles separation $\boldsymbol{R}$. At very small separations $R \ll l_\eta$ we have that the velocity difference in (28) can be reasonably approximated by a linear expansion in R, which in most time-dependent flows leads to an exponential growth of the separation of initially close particles, i.e.

$$\langle \ln R(t) \rangle \simeq \ln R(0) + \lambda t \,, \tag{29}$$

where the average is taken over many couples with initial separation $R(0)$, and λ is the Lagrangian Lyapunov exponent. The rigorous definition of the Lyapunov exponent imposes to take the two limits $R(0) \to 0$ and then $t \to \infty$: in physical terms these limits amount to the requirement that the separation, for very large times, has not to exceed l_η. This is a very strict condition, rarely accomplished in real flows, rendering often difficult the experimental observation of (29).

On the opposite limit, for very long times and for separations $R \gg L_0$, the two trajectories $\boldsymbol{x}_1(t)$ and $\boldsymbol{x}_2(t)$ feel two uncorrelated velocities and we expect normal diffusion, i.e.

$$\langle R^2(t) \rangle \simeq 4D^E \, t \,, \tag{30}$$

the factor 4 is due to the fact that the two particles are asymptotically independent.

Between the two asymptotic regimes (29) and (30) the behavior of $R(t)$ depends on the particular flow. For instance, as we shall see, if the flow is turbulent with $\delta_R v \sim R^{1/3}$ an anomalous relative dispersion process takes place, i.e.

$$\langle R^2(t) \rangle \sim t^3 \,, \tag{31}$$

which is the celebrated Richardson dispersion.

In realistic settings however the characteristic length-scales are not sharply separated, and the description of dispersion in terms of asymptotic quantities is infeasible, and different approaches are needed.

2.5 Scale-by-scale description of dispersion

To treat the difficulties due to the lack of asymptotic let us now introduce a scale dependent description of dispersion. Consider a particle pairs advected by a smooth velocity field with characteristic length l_η. Assuming that the Lagrangian motion is chaotic, we expect the following regimes:

$$\langle R^2(t) \rangle \simeq \begin{cases} R_0^2 \exp(\Lambda(2)t) & \text{if } \langle R^2(t) \rangle^{1/2} \ll l_\eta \\ 4D^E t & \text{if } \langle R^2(t) \rangle^{1/2} \gg l_\eta \end{cases} \,, \tag{32}$$

where $\Lambda(2) \geq 2\lambda$ is the generalized Lyapunov exponent [38], D^E is the effective diffusion coefficient for the single particles dispersion. The regimes (32) can be seen only in the asymptotic limits $t \ll 1/\lambda$ and $t \gg 1/\lambda$, respectively. The presence of fluctuations in the rate of particles separation, which is characterized in terms of the finite time Lyapunov exponents [7], will easily determine situations such that at the same time different couples are in the two different regimes. Therefore, as consequence of this "contamination", crossovers with spurious regime are generically present (see e.g. Fig. 1 in Ref.[39]). This comes essentially because we considered the "wrong" variable, i.e., the time instead of the physical one, i.e., the scale.

A possibility for characterizing the dispersion properties in terms of the scale is by introducing the "doubling time" $\tau(\delta)$ at scale δ as follows [38, 39]: given a series of thresholds $\delta^{(n)} = r^n \delta^{(0)}$, one can measure the time $T_i(\delta^{(0)})$ it takes for the separation $R(t)$ to grow from $\delta^{(0)}$ to $\delta^{(1)} = r\delta^{(0)}$, and so on for $T_i(\delta^{(1)})\,,\ T_i(\delta^{(2)})\,,\ldots$ up to the largest considered scale. The r factor may be any value larger than 1, properly chosen in order to have a good separation between the scales of motion, i.e. r should be not too large. Strictly speaking, $\tau(\delta)$ is exactly the doubling time if $r = 2$. Then performing the doubling time experiments over $\mathcal{N}$ particle pairs separation experiments, the average doubling time $\tau(\delta)$ at scale δ is defined as

$$\tau(\delta) =< T(\delta) >_e = \frac{1}{\mathcal{N}} \sum_{i=1}^{\mathcal{N}} T_i(\delta)\,, \tag{33}$$

notice that this average is different from the usual time average.

Now we can define the Finite Size Lyapunov Exponent (FSLE) [38, 39] in terms of the average doubling time

$$\lambda(\delta) = \frac{\ln r}{\tau(\delta)}\,, \tag{34}$$

which quantifies the average rate of separation between two particles at a distance δ. For very small separations (i.e. $\delta \ll l_\eta$) one recovers the Lagrangian Lyapunov exponent $\lambda = \lim_{\delta\to 0} \ln r/\tau(\delta)$. At large separation the diffusive behavior is signaled by the fact that $\tau(\delta) \sim \delta^2$. Thus the finite size Lagrangian Lyapunov exponent $\lambda(\delta)$ behaves as follows:

$$\lambda(\delta) \sim \left\{ \begin{array}{ll} \lambda & \text{if } \delta \ll l_\eta \\ 2D^E/\delta^2 & \text{if } \delta \gg l_\eta \end{array} \right. , \tag{35}$$

One could naively conclude, matching the behaviors at $\delta \sim l_\eta$, that $D^E \sim \lambda l_\eta^2$. This is not always true, since one can have a rather large range for the crossover due to nontrivial correlations which can be present in the Lagrangian dynamics [7, 39]. One can also define a sort of scale dependent diffusion coefficient as $D(\delta) = \delta^2 \lambda(\delta)$.

One might wonder that the introduction of $\tau(\delta)$ is just another way to look at $\langle R^2(t)\rangle$. This is true only in limiting cases, when the different characteristic lengths are well separated and intermittency is weak. Examples of the usefulness of this indicator may be found in Refs. [39, 40, 41].

2.6 Pair dispersion in laminar flows in presence of boundaries

In the case of flows confined in finite domains having size L_B in addition to the two asymptotic regimes (35), another regime appear. For separations close to the average maximal allowed separation $\delta_{max} \simeq L_B$, the following behavior holds for a broad class of systems [7]:

$$\lambda(\delta) = \frac{D(\delta)}{\delta^2} \propto \frac{1}{\tau_R} \frac{(\delta_{max} - \delta)}{\delta}\,, \tag{36}$$

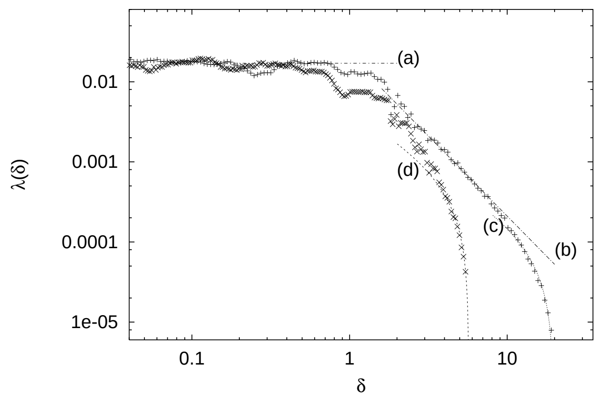

Figure 4: $\lambda(\delta)$ vs δ for the flow (24) with: $\psi_0 = 0.2,\ B = 0.4,\ \omega = 0.4$. Particle motion has been confined in closed domain with 6 (crosses) and 12 (diamonds) convective cells, respectively. $\lambda(\delta)$ has been computed with $\mathcal{N} = 2000$ realization. As for the thresholds we used $\delta_n = \delta_0 r^n$ with $\delta_0 = 10^{-4}$ and $r = 1.05$. The lines are respectively: (a) Lyapunov regime with $\lambda = 0.017$; (b) diffusive regime with $D^E = 0.021$; (c) saturation regime with $\delta_{max} = 19.7$; (d) saturation regime with $\delta_{max} = 5.7$.

where τ_R is related to the exponential relaxation of the distribution of particles inside the domain to the uniform distribution which is always attained at long times (see [7] for more details).

To exemplify the scale dependence of $\lambda(\delta)$, let us reconsider again the flow (24) where now, to study the effects of finite boundaries, we confine the tracers' motion in a finite domain. To this aim we slightly modified the oscillating term in (24) as $B \to B \sin(\pi x/L_B)$ with $L_B = 2\pi n/k$ (n is the number of convective cells). In this way the motion is confined in $x \in [-L_B, L_B]$. In Figure 4 we show $\lambda(\delta)$ for two values of L_B. If L_B is large enough one can distinguish the three regimes: exponential (if δ is much smaller than the cell), diffusive (at scales larger than the unit cell) and the saturation regime eq. (36) (for separation close to the system size). Decreasing L_B, the range of the diffusive regime decreases, and for small values of L_B, it disappears.

Let us now discuss the use of the FSLE for the analysis of experimental Lagrangian data in a convective flow [42]). The experimental apparatus is a rectangular convective tank $L = 15.0\,cm$ wide, $10.4\,cm$ deep and $H = 6.0\,cm$ height filled with water. The upper and lower surfaces are kept at constant temperature and the side walls can be considered as adiabatic. Convection is by an electrical circular heater, $0.8\,cm$ in diameter, located in the mid-line of the tank, just above the lower surface (Fig. 5). The heather furnishes a constant heat flux controlled by a feedback on the power supply. The control parameter of the experiment is the Rayleigh number, Ra, which is varied over a wide range of values. The geometrical configuration constrains the convective pattern to two counter-rotating rolls divided by a oscillating thermal plume (see Fig. 5 for a view of the typical Lagrangian motion). The Eulerian velocity field is thus, basically, two-dimensional and time periodic.

Lagrangian data are obtained by Particle Tracking Velocimetry (PTV) tech-

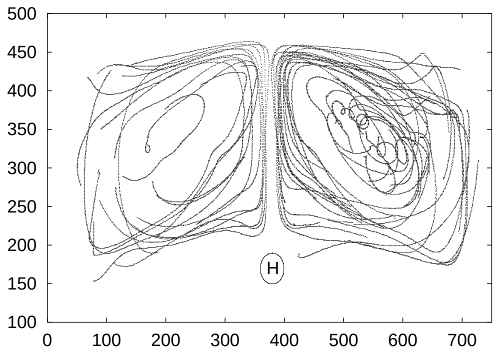

Figure 5: An example of trajectories reconstructed by the PVT technique (unit in pixels). The circle on the bottom represents the heater.

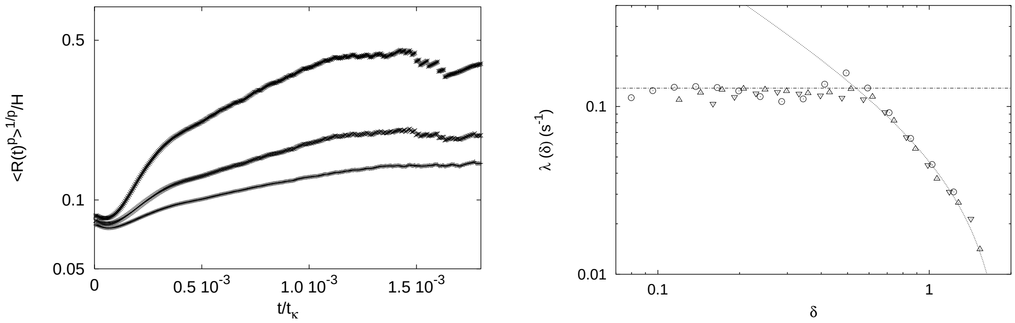

Figure 6: (left) Rescaled relative dispersion $\langle R(t)^p \rangle^{(1/p)}$ for $p = 1, 2, 4$ (from bottom to top) in lin-log plot, for the run at $Ra = 2.39\,10^8$. The dependence of the slope on the order p is an indication of the strong intermittency in the Lagrangian separation. Time is rescaled in terms of the diffusion time. (right) $\lambda(\delta)$ versus δ in the same run. Different initial threshold $\delta_0 = 0.4\,cm$ ($\circ$), $\delta_0 = 0.6\,cm$ ($\triangle$) and $\delta_0 = 0.8\,cm$ ($\bigtriangledown$) have been considered to test the statistical robustness of the measure. The straight line is the Lyapunov exponent $\lambda = (0.12 \pm 0.01)s^{-1}$ and the curve represents the saturation regime (36).

nique [43]. In Figure 6 (left) we show moments of the relative separation between particles, $\langle R^q(t) \rangle^{1/q}$ versus t for the run at $Ra = 2.39\,10^8$ computed over about 900 trajectories. As one can see it is very difficult to extract any reliable behavior from this observable. On the other had from the FSLE reported in Fig. 6 (right) it is rather clear what is happening. For small δ, we observe the collapse of $\lambda(\delta)$ to the value of the Lyapunov exponent, independent on δ_0. For larger separation $\lambda(\delta)$ decreases to smaller values, indicating a slowing down in the separation growth due to the presence of boundaries. The behavior of $\lambda(\delta)$ is indeed well described by the prediction (36). The absence of a diffusive regime is due to the fact that the size of Eulerian structure is of the same order of the tank size.

2.7 Pair dispersion in turbulent flows

Let us now consider the pair dispersion properties in fully developed turbulent velocity fields. In this case we have that the velocity increments are approximately well described by Kolmogorov 1941 theory

$$\delta_R v \sim R^h \qquad h = 1/3 \,. \tag{37}$$

Actually real turbulent flows are intermittent and cannot be described in terms of a single exponent h [37]. However, let us for the moment neglect such fluctuations and treat the flow as if it is self-similar with $h = 1/3$. Furthermore let us assume that $l_\eta \to 0$, i.e. that the velocity field is turbulent up to the smallest available scale. Of course, this is a very idealized situations which is only approximately true in realistic turbulent flows.

The first important observation is that at variance with smooth velocities (i.e. $\delta_r v \sim r$) where in the limit of zero diffusivity particle trajectories are unique, if $\boldsymbol{v}$ is rough (i.e. $h < 1$) Lagrangian paths are not unique and also initially coincident particles separate. This is exemplified as follows. Let R be the separation between two particles, its temporal evolution (modeled in one-dimension for simplicity) is given by $dR/dt = \delta_R v \propto R^{1/3}$ and $R(0) = R_0$. Then for $R_0 > 0$, the solution is given by

$$R(t) = \left[R_0^{2/3} + \frac{2}{3}t\right]^{3/2} \,. \tag{38}$$

If $R_0 = 0$ two solutions are allowed, i.e. $R(t) = [\frac{2}{3}t]^{3/2}$ and the trivial one $R(t) = 0$: trajectories are not unique. Physically this means that for $R_0 \neq 0$ the solution becomes independent of the initial separation R_0, provided t is large enough. More interestingly one has that trajectories separate anomalously

$$\langle R^2(t)\rangle \sim t^3 \,, \tag{39}$$

as one easily obtains from (38). This is the well known Richardson law for particles dispersion in turbulent flows [44, 6]. Of course, in realistic flows one should expect that this regime ends at time such that $\langle R(t)\rangle \sim L_0$, and, in absence of boundaries, the standard diffusive behavior will establish at larger times. It is worth mentioning that the mechanism underlying this "anomalous" diffusive behavior is the same as the one discussed in the context of single particle diffusion: the Lagrangian velocity differences correlation function does not decay when particle separation is within the inertial range so that conditions for the validity of the standard diffusion discussed in Sect. 2.1 are violated (see, e.g., Ref. [3]).

Similarly to absolute dispersion one can describe the relative dispersion in terms of the probability of finding particle's pairs at separation R at time t, i.e. $p(R, t)$, actually this was the path originally proposed by Richardson. The Richardson law can be obtained assuming that the diffusion coefficient is scale dependent $D = D(R)$. Actually this can be physically justified as follows: the dimension of D are $(time)^{-1}$ $(scale)^2$ using $R/\delta_R v$ and R as the proper time and scale, respectively one obtains $D(R) \sim R^{4/3}$. Therefore in d-dimensions, in spherical coordinates, one has that $p(R, t)$ obeys the equation

$$\partial_t p(R,t) = \frac{1}{R^{d-1}} \left(\frac{\partial}{\partial_R} R^{d-1} D(R) \frac{\partial}{\partial_R} p(R,t)\right) \,. \tag{40}$$

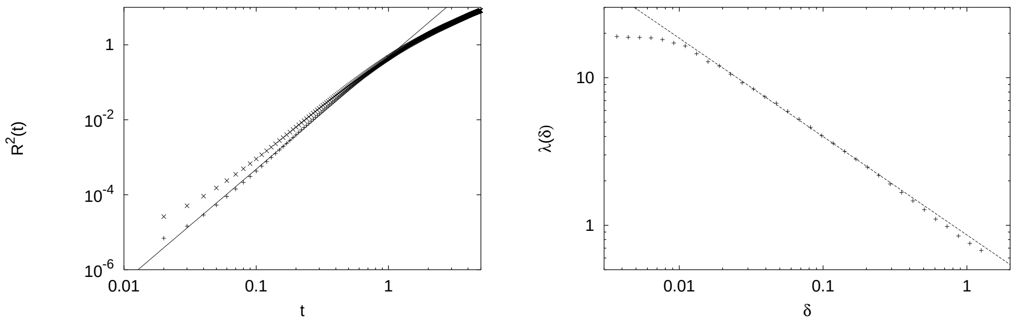

Figure 7: (left) Relative dispersion $\langle R^2(t)\rangle$ for two initial separation $R(0) = 1.5\times10^{-3}$ (+) and $R(0) = 3\times10^{-3}$ ($\times$). The continuous line is the Richardson law $R^2(t) \simeq t^3$. (right) Finite Size Lyapunov Exponent $\lambda(\delta)$ in the same simulation. The initial threshold is $\delta_0 = 0.0031$ and the ratio is $r = 1.2$. The line is the theoretical Richardson scaling $\delta^{-2/3}$.

Although the argument which lead to the above equation is very rough, one can prove that if the velocity field is rapidly decorrelating in time Eq. (40) is indeed exact [3]. Eq. (40) is solved by

$$p(R,t) \sim \frac{R^{d-1}}{t^{3d/2}} e^{-c\frac{R^{2/3}}{t}} \tag{41}$$

which gives the Richardson law $\langle R^2\rangle = \int dR R^2 p(R,t) \propto t^3$. Moreover, note that $p(R,t) = t^{-3/2}F(t^{-3/2}R)$ consistently with (21), indeed the assumption of a perfect scale-invariance for the velocity field leads to a "weak" anomalous behavior, i.e. $\langle R^q\rangle \sim t^{3/2q}$. This can be considered a good approximation for two-dimensional turbulent flows in the inverse energy cascade regime [45].

In Fig. 7 we report the results of Boffetta and Celani [46] for Richardson diffusion in two-dimensional turbulence. Fig. 7 (left) shows the behavior of $\langle R^2(t)\rangle$ vs time. Note that, notwithstanding the high numerical resolution of the simulation, the presence of large crossovers makes the t^3 law not easily detectable. In fact, as follows also from Eq. (38) the memory of the initial separation is only asymptotically recovered. On the other hand Fig. 7 (right) reports the computation of the FSLE in the same simulation, as one can see the Richardson law is much more evident as signaled by the scaling $\lambda(\delta) \sim \delta^{-2/3}$. Actually the same qualitative picture persists also in synthetic turbulent flows where the resolution can be enhanced a lot (see, e.g., Refs.[45]). In realistic turbulent flows, assuming that all the scales can be resolved the following regime for the FSLE should be expected: $\lambda(\delta) = \lambda$ for $\delta \ll l_\eta$; $\lambda(\delta) \sim \delta^{-2/3}$ for $l_\eta \ll \delta \ll L_0$; $\lambda(\delta) \sim \delta^{-2}$ for $\delta \gg L_0$.

Finally in Fig. 8 the prediction (41) is compared with the numerical results, showing that at least for the case of two-dimensional Navier-Stokes turbulence the Richardson description is a good approximation even if the velocity field has non trivial correlations and does not rapidly decorrelate.

For three dimensional turbulent flows one has to consider that the are fluctuations in the local roughness exponents h (see Eq. 37). This of course will modify the properties of the relative dispersion. Actually, different moments of

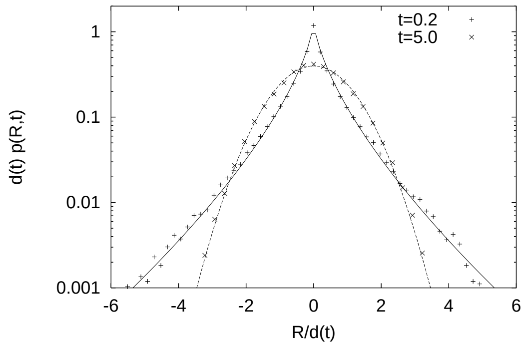

Figure 8: Probability density function of relative separation at times $t = 0.2$ and $t = 5.0$ rescaled with $d(t) = \langle R^2(t)\rangle^{1/2}$. The continuous line is the Richardson prediction (41), the dashed line is a Gaussian distribution. At large time the Gaussian behavior is recovered.

the separation scale with exponents different from the dimensional prediction: $\langle R^q\rangle \neq t^{3/2q}$. However, in the framework of the multifractal model of turbulence still one can show that for $q = 2$ the Richardson law holds. We refer the reader to Ref. [47] where evidences for such deviations have been found both in synthetic turbulent flows and DNS of three dimensional turbulence.

3 Transport of reacting substances

We consider the case of a unique scalar reactive field $\theta(\mathbf{x}, t)$. This model is appropriate in aqueous auto-catalytic premixed reactions, and gaseous combustion with a large flow intensity but low value of gas expansion across the flame [8]. The field θ evolves according to the advection-reaction-diffusion (ARD) equation:

$$\partial_t\theta + (\mathbf{u}\cdot\boldsymbol{\nabla})\theta = D\Delta\theta + \frac{1}{\tau}f(\theta)\,, \tag{42}$$

where $f(\theta)$ accounts for the reaction and τ is reaction characteristic time [8, 14, 15, 16]. For the sake of simplicity, we take $f(\theta) = \theta(1-\theta)$. However, the results we are going to describe do not depend on the specific form of $f(\theta)$ provided that $f(\theta)$ is convex ($f''(\theta) < 0$) and positive in the interval $(0, 1)$, vanishing at its extremes, and $f'(0) = 1$. This corresponds to the FKPP type of reaction [10, 11].

In Sect. 2 we saw the link between the solution of Eq. (2) and Lagrangian trajectories. There exist a similar relation also for Eq. (42) [48]:

$$\theta(\boldsymbol{x}, t) = \left\langle \theta(\boldsymbol{x}(0), 0)\, \exp\left(\frac{1}{\tau}\int_0^t \frac{f(\theta(\boldsymbol{x}(s;t), s))}{\theta(\boldsymbol{x}(s;t), s)}\mathrm{d}s\right)\right\rangle\,, \tag{43}$$

where the average is performed over all the trajectories $\boldsymbol{x}(s;t)$ that ended in $\boldsymbol{x}(t;t) = \boldsymbol{x}$ (as in (7)).

Using the maximum principle [48] and noting that $f(\theta)/\theta \le f'(0)$, because of the convexity of $f(\theta)$, one can write an upper bound for $\theta(\mathbf{x}, t)$ in terms of the solution, $\theta_L(\mathbf{x}, t)$, of the linearized ARD:

$$\partial_t\theta_L + (\mathbf{u}\cdot\boldsymbol{\nabla})\theta_L = D\Delta\theta_L + \frac{f'(0)}{\tau}\theta_L\,. \tag{44}$$

In fact, if $\theta(\mathbf{x},0) \leq \theta_L(\mathbf{x},0)$ one has [48]

$$\theta(\mathbf{x},t) \leq \theta_L(\mathbf{x},t) \tag{45}$$

From Eq.s (43-45) one obtains

$$\theta(\mathbf{x},t) \leq \langle \theta(\mathbf{r}(0),0) \rangle \exp\left(\frac{f'(0)}{\tau} t \right) . \tag{46}$$

The right hand side of the previous equation is the solution of Eq. (44) and, in particular, $\langle \theta(\mathbf{r}(0),0) \rangle$ is nothing but the solution $P(\mathbf{x},t)$ at time t of the passive scalar PDE (2) with initial condition $\theta(\mathbf{x},0)$ (that we suppose localized around $\mathbf{x}=0$).
In Sect. 2.1 we saw that under general conditions (i.e. spatial and temporal short-range correlations) Eq. (2) has the same asymptotic behavior of a Fick equation. As a consequence, we have

$$< \theta(\mathbf{r}(0),0) > \equiv P(\mathbf{x},t) \sim \frac{1}{\sqrt{2\pi D^E_{11} t}} \exp\left(-\frac{x^2}{4 D^E_{11} t} \right) . \tag{47}$$

Eq.s (46) and (47) imply that, along the x-direction, the field θ is exponentially small until a time t of the order of $x/\sqrt{4 D^E_{11} f'(0)/\tau}$, therefore an upper bound for v_f comes out

$$v_f \leq 2\sqrt{D^E_{11} f'(0)/\tau} . \tag{48}$$

The above discussion shows that, if standard diffusion holds, then there is a front propagating with a constant speed, i.e., there is not qualitative difference with respect to the solvable case $\mathbf{u}=0$. Nevertheless, the analytical determination of v_f, for a given velocity field, $\mathbf{u}$, is a rather difficult problem even for simple laminar fields [14, 15, 16, 18]

3.1 Fronts in cellular flows

The bound (48) is very general and holds for generic incompressible flows and production terms. Here we numerically investigate the properties of front propagation in the particular case of the cellular flow (24). This kind of flow is interesting because, at variance with shear flows, all the streamlines are closed and, therefore, the front propagation is determined by the mechanisms of contamination of one cell to the other [14, 16]. As first we consider the time-independent case, i.e. $B=0$ in (24). Since we are interested in the propagation in the x-direction we take periodic boundary conditions in y and an infinite extent along the x-axis with boundary conditions $\theta(-\infty,y;t)=1$ and $\theta(+\infty,y;t)=0$.

The bulk burning rate,

$$v_{\mathrm{f}}(t) = \frac{1}{L}\int_0^L \mathrm{d}y \int_{-\infty}^{\infty} \mathrm{d}x\, \partial_t \theta(x,y;t) , \tag{49}$$

coincides with the front speed when the latter exists, but it is also a well defined quantity even when the front itself is not well defined. The asymptotic (average) front speed, v_{f}, is determined by $v_{\mathrm{f}} = \lim_{T\to\infty} 1/T \int_0^T \mathrm{d}t\, v_{\mathrm{f}}(t)$.

In our discussion, we always suppose that the diffusion time scale is the slowest one and thus $Pe \gg 1$ and $Da \cdot Pe \gg 1$.

On large scales and long times the effects of the velocity field can be modeled in terms of reaction-diffusion process with renormalized coefficients [14],

$$\partial_t \theta = D^E \Delta\theta + \frac{1}{\tau_{\rm eff}} F(\theta)\,, \tag{50}$$

The renormalized diffusivity D^E accounts for the process of diffusion from cell to cell as a result of the nontrivial interaction of advection and molecular diffusion [6]. The renormalized reaction time $\tau_{\rm eff}$ is the time it takes for a single cell to be filled by inert material, and depends on the interaction of advection and production. Therefore, the limiting speed of the front in the moving medium is given by $v_{\rm eff} \sim \sqrt{D^E/\tau_{\rm eff}}$ [14, 15]. The problem is now reduced to derive the expressions for the renormalized parameters by means of physical considerations.

In the following sections, using as an interpretative framework the above described macroscopic model, we will present the results of detailed numerical simulations for slow ($Da \ll 1$) and fast ($Da \gg 1$) reaction.

3.2 Slow and fast reaction regimes

The renormalized characteristic time can be extimated as follows. At small Da, the reaction is significantly slower than the advection, and consequently the region where the reaction takes place extends over several cells, i.e., the front is distributed. The dependence of D^E on Pe and D is a well studied problem, the solution of which is [6]:

$$\frac{D^E}{D} \sim Pe^{1/2} \qquad Pe \gg 1\,. \tag{51}$$

Therefore, in the slow reaction regime, $Da \ll 1$, a single cell is first invaded by a mixture of reactants and products (on the fast advective time scale), and subsequently complete reaction is achieved on the slower time scale $\tau_{\rm eff} \simeq \tau$ (see Fig. 9). In the case of fast reaction, $Da \gg 1$, two sharply separated phases emerge inside the cell and the filling process is characterized by an inward spiral motion of the outer, stable phase (see Fig. 9), at a speed proportional to U. Therefore we have

$$\frac{\tau_{\rm eff}}{\tau} \sim \begin{cases} 1 & Da \ll 1 \\ Da & Da \gg 1\,. \end{cases} \tag{52}$$

From (51) and (52) we can derive the front speed for a cellular flow. Indeed, recalling that $v_{\rm f} \sim \sqrt{D^E/\tau_{\rm eff}}$, we have [14, 15]

$$\frac{v_{\rm f}}{v_0} \sim \begin{cases} Pe^{1/4} & Da \ll 1\,,\ Pe \gg 1 \\ Pe^{1/4} Da^{-1/2} & Da \gg 1, Pe \gg 1 \end{cases} \tag{53}$$

The case of $Pe \ll 1$ is less interesting because the dynamics is dominated by diffusion.

In terms of the typical velocity of the cellular flow, we have $v_{\rm f} \propto U^{1/4}$ for slow reaction ($U \gg L/\tau$, or equivalently $Da \ll 1$) whereas $v_{\rm f} \propto U^{3/4}$ for fast

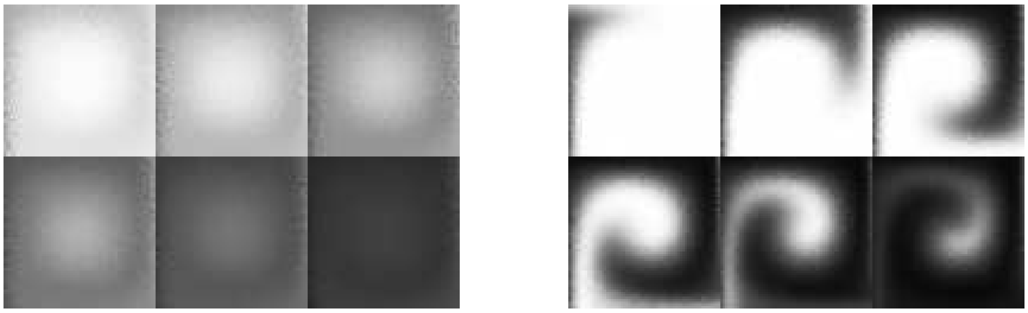

Figure 9: (left)Six snapshots of the field θ within the same cell, at six successive times with a delay $\tau/6$ (from left to right, top to bottom), as a result of the numerical integration of equation (42). Here $Da \simeq 0.4, Pe \simeq 315$. Black stands for $\theta = 1$, white for $\theta = 0$. (right) The same but for $Da = 4, Pe = 315$, τ is now replaced by $\tau_{eff} \sim L/U$. Note that a spiral wave invades the interior of the cell, with a speed comparable to U.

reaction ($U \ll L/\tau$, or $Da \gg 1$). The scaling $v_{\rm f} \propto U^{1/4}$ for slow reaction (i.e. fast advection) is a consequence of $D^E \propto DPe^{1/2}$ [6] in the homogenization limit [14, 15], it has been obtained in [14, 16]. To check these ideas, we performed numerical simulations of Eq. (42), with a FKPP production term. The numerical results are summarized in Fig. 10.

As a remark we mention that, for the class of boundary conditions investigated here, where the region of initially burnt material extends to infinity, no quenching [15] takes place no matter of the used production term. Numerical simulations show that Arrhenius-type nonlinearity gives the same qualitative results as those of FKPP-type reaction presented above, i.e., one has the two scaling laws $v_{\rm f} \propto U^{1/4}$ and $v_{\rm f} \propto U^{3/4}$ at fast and slow advection respectively [14].

3.3 Geometrical optics limit

When the front thickness and the reaction time are much smaller than the length and time scales of the velocity field fluctuations one has the geometrical optics regime. Mathematically speaking this regime is realized for $(D, \tau) \to 0$ maintaining D/τ constant [18, 49]. In this limit one has a non zero bare front speed, v_0, while the front thickness ξ goes to zero, i.e., the front is sharp.

The sharp interface separating the reactants from the products is modeled by the G-equation (54) [9, 49]:

$$\frac{\partial G}{\partial t} + \mathbf{u} \cdot \boldsymbol{\nabla} G = v_0 |\boldsymbol{\nabla} G| \,. \tag{54}$$

The front is defined by a constant level surface of the scalar function $G(\mathbf{r}, t)$.

As far as the cellular flow is concerned, the front border is wrinkled by the velocity field during propagation and its length increases until pockets of fresh material develop [50, 51] (see Fig. 11). After this, the front propagates periodically in space and time with an average speed $v_{\rm f}$, which is enhanced with respect to the propagation speed v_0 of the fluid at rest.

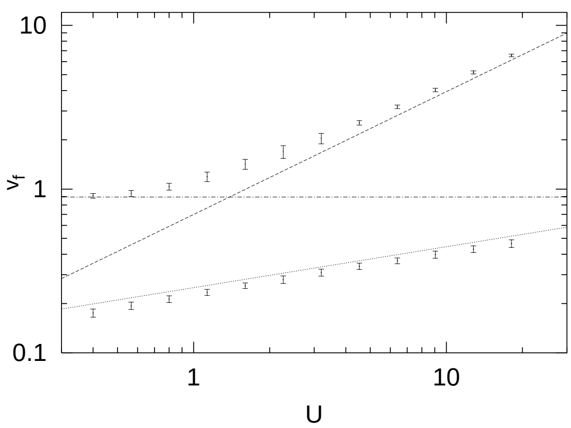

Figure 10: The front speed v_{f} as a function of U, the typical flow velocity. The lower curve shows data at $\tau = 20.0$ (fast advection). The upper curve shows data at $\tau = 0.2$ (slow advection). For comparison, the scalings $U^{1/4}$ and $U^{3/4}$ are shown as dotted and dashed lines, respectively. The horizontal line indicates v_0, the front velocity without advection, for $\tau = 0.2$.

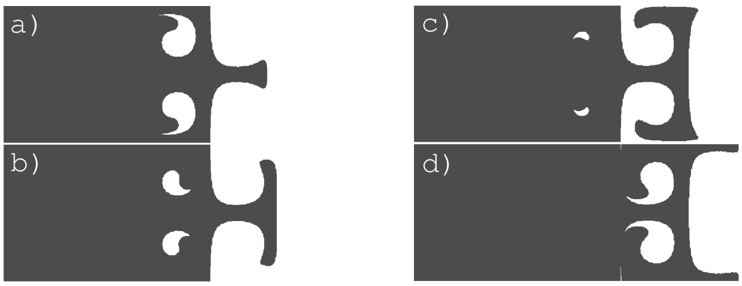

Figure 11: Snapshot of the front shape with time step $T/8$ (from (a) to (d)), where T is the period of the front dynamics, for $v_0 = 0.5$, $U = 4.0$ and $L = 2\pi$. Unburnt (burnt) material is indicated in white (black).

Let us now consider the flow (24) with $B = 0$, i.e., the stationary case. The problem addressed here is the dependence of the effective speed v_{f} on the flow intensity, U, and the bare velocity, v_0, that is expected of the form [52]:

$$\frac{v_{\mathrm{f}}}{v_0} = \psi\left(\frac{U}{v_0}\right) , \tag{55}$$

where $\psi(\mathcal{U})$ is a function which depends on the flow details.

As far as we know, apart from very simple shear flows (for which $\psi(\mathcal{U}) = 1+\mathcal{U}$ [53]), there are no methods to compute $\psi(\mathcal{U})$ from first principles. Mainly one has to resort to numerical simulations and phenomenological arguments.

For turbulent flows, by means of dynamical renormalization group techniques, Yakhot [54] proposed

$$\frac{v_{\mathrm{f}}}{v_0} = e^{(U/v_{\mathrm{f}})^{\alpha}} \tag{56}$$

with $\alpha = 2$, now U indicates the root mean squared average velocity (see also [55, 56]). Therefore, from (56) one has that $v_{\mathrm{f}} \to U/\sqrt{\ln(U)}$ for $U \to \infty$.

For the cellular flow under investigation, albeit the exact form of the function $\psi(\mathcal{U})$ is not known, a simple argument can be given for an upper and a lower bound by mapping the front dynamics onto a one-dimensional problem. The starting point is the following observation. In the optical regime, since the interface is sharp, i.e., $\theta(x, y)$ is a two-valued function ($\theta = 1$ and $\theta = 0$), we can track the farther edge of the interface between product and material $(x_M(t), y_M(t))$, which is defined as the rightmost point (in the x-direction) for which $\theta(x_M, y_M; t) = 1$. Then we can define a velocity

$$\tilde{v}_f = \lim_{t\to\infty} \frac{x_M(t)}{t} , \tag{57}$$

which gives an equivalent value of the standard definition (49). After a transient, in the unit cell $[0, 2\pi]$ (we describe the case $L = 2\pi$) the point $(x_M(t), y_M(t))$ moves to the right along the separatrices of the streamfunction (24), so that $y_M(t)$ is essentially close to the values 0 or π. Along this path one can reduce the edge dynamics to the $1d$-problem

$$\frac{\mathrm{d}x_M}{\mathrm{d}t} = v_0 + U\beta|\sin(x_M(t))| \tag{58}$$

where the second term of the r.h.s. is the horizontal component of the velocity field. We have neglected the y-dependence, replacing it with a constant β which takes into account the average effect of the vertical component of the velocity field along the path followed by (x_M, y_M). By solving (58) in the interval $x_M \in (0, 2\pi)$ one obtains the time, T, needed for x_M to reach the end of the cell. The front speed, as the speed of the edge particle, is then given by $v_{\mathrm{f}} = 2\pi/T$. The final result is

$$\frac{v_{\mathrm{f}}}{v_0} = \psi_\beta(\mathcal{U}) = \frac{\pi\sqrt{(\mathcal{U}\beta)^2 - 1}}{2\ln\left(\mathcal{U}\beta + \sqrt{(\mathcal{U}\beta)^2 - 1}\right)} , \tag{59}$$

Note that (59) is valid only for $\mathcal{U}\beta \geq 1$.

We have taken $\beta = 1$ for the upper bound and $\beta = 1/2$ (which is the average of $|\cos(y)|$ between 0 and π) for the lower bound. We have also computed the

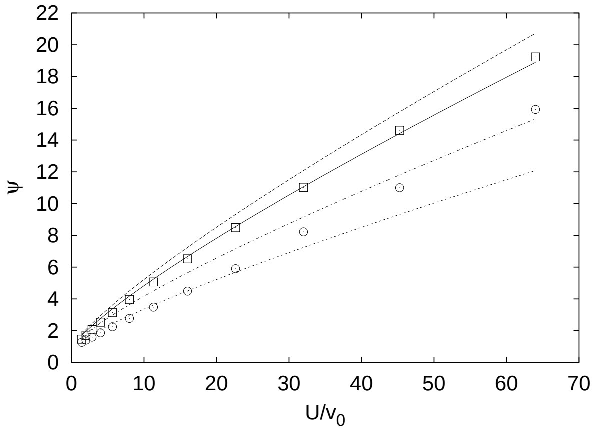

Figure 12: The measured $\psi(U/v_0)$ as a function of U/v_0 ($\square$), the Yakhot formula (56) with $\alpha = 2$ (o), the function ψ_β for $\beta = 1, 1/2$ (dashed and dotted lines) and for $\beta = 0.89$ (solid line). The dashed-dotted line is the bound (60).

average of $|\cos(y_M(t))|$ in a period of its evolution obtaining $\beta \approx 0.89$ which gives indeed a very good approximation of the measured curve (see Fig. 12). We stress that the theoretical curve is not a fit, but it just involves the measured parameter β.

This agreement is an indication that the average of $|\cos(y_M(t))|$ depends on U and v_0 very weakly (as we checked numerically). Previous studies [55, 56] reported an essentially linear dependence of the front speed on the flow intensity, i.e., $v_{\mathrm{f}} \propto U$ for large U which is not too far but different from our result. A rigorous bound has been obtained in Ref [57] by using the G-equation:

$$v_{\mathrm{f}} \geq U/(\log(1 + U/v_0)) \ . \qquad (60)$$

As one can see from Fig. 12, the lower bound (60) seems to be closer to the numerical data than the one obtained with $\beta = 1/2$ in (59). From Eq. (59), asymptotically (i.e. for $U \gg v_0$) one has: $v_{\mathrm{f}} \sim U/\ln(U)$ which corresponds to (56) for $\alpha = 1$. Expressions as (56) have been proposed for flows with many scales as, e.g., turbulent flows, and in the literature different values of α have been reported [54, 55, 56]. The fact that also the simple one-scale vortical flow investigated here displays such a behavior may be incidental. However, we believe that it can be due to physical reasons. Indeed, the large scale features of the flow, e.g. the absence of open channels (like for the shear flow) can be more important than the detailed multi-scale properties of the flow [50].

3.4 Is chaos important?

An interesting problem is the thin front dynamics in the presence of Lagrangian chaos generated by the time periodic streamfunction (24). We are mainly interested in addressing the two following issues. First, since trajectories starting near the roll separatrices typically have a positive Lyapunov exponent, it is natural to wonder about the role of Lagrangian chaos on front propagation. Second, as we have shown in Sect. 2.3, we know that for the time dependent streamfunction

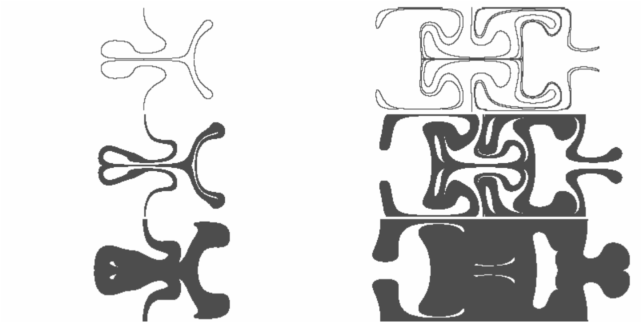

Figure 13: Snapshots at two successive times, $t = 3.6$ and 7.5, of the evolution of passive (top) and reactive line of material for two values of v_0 (middle $v_0 = 0.7$ and bottom $v_0 = 2.1$) for $U = 1.9$, $B = 1.1$ and $\omega = 1.1U$. The initial condition is a straight vertical line.

(24) the transport properties are strongly enhanced, therefore it is worth to see if similar effects are reflected also in the front speed.

In order to define the instantaneous front length, $\mathcal{L}(t)$, we introduce the variable $\sigma_\epsilon(x, y; t)$ which assumes the value 0 if θ is constant inside a circle of radius ϵ centered in (x, y) at time t, otherwise $\sigma_\epsilon(x, y; t) = 1$ (i.e., $\sigma_\epsilon(x, y; t) = 1$ only if the ϵ-ball centered in (x, y) contains a portion of the front). The front length is then defined by

$$\mathcal{L}(t) = \lim_{\epsilon \to 0} \frac{1}{\epsilon} \int_{-\infty}^{\infty} \mathrm{d}x \int_0^L \mathrm{d}y \, \sigma_\epsilon(x, y; t) \ . \tag{61}$$

A direct consequence of Lagrangian chaos is the exponential growth of passive scalar gradients and material lines [1, 4]: a (passive) material line of initial length ℓ_0 for large times grows as

$$\ell(t) \sim \ell_0 e^{\Lambda(1)t} \, . \tag{62}$$

Where $\Lambda(1)$ is the generalized Lyapunov exponent, $\Lambda(1) \geq \lambda$ [38]. In the presence of molecular diffusivity, the exponential growth of $\ell(t)$ stops due to diffusion and chaos is just a transient [58]. For reacting scalars something very similar happens. Let us compare the evolution of material lines in the passive and reactive cases (see Fig. 13). While in the passive case (without molecular diffusivity) structures on smaller and smaller scales develop (due to stretching and folding), in the reactive systems after a number of folding events structures on smaller scales are inhibited as a consequence of the Huygens dynamics: the interface between the two phases merges. This phenomenon is responsible for the formation of *pockets*. Of course, "merging" is more and more efficient as v_0 increases (compare the middle and lower pictures of Fig. 13).

In Fig. 14 we show the time evolution of the line length, $\mathcal{L}(t)$, as a function of t for the passive and reactive material at different values of v_0. While at small times both the passive and reactive scalar lines grow exponentially with a rate close to $\Lambda(1)$, at large time $t > t^*$ (where t^* is a transient time depending on v_0) the reacting ones stops due to merging. Asymptotically, the front length varies periodically with an average value depending on v_0. A rough argument to estimate t^*, is the following: two initially separated part of the line (e.g.,

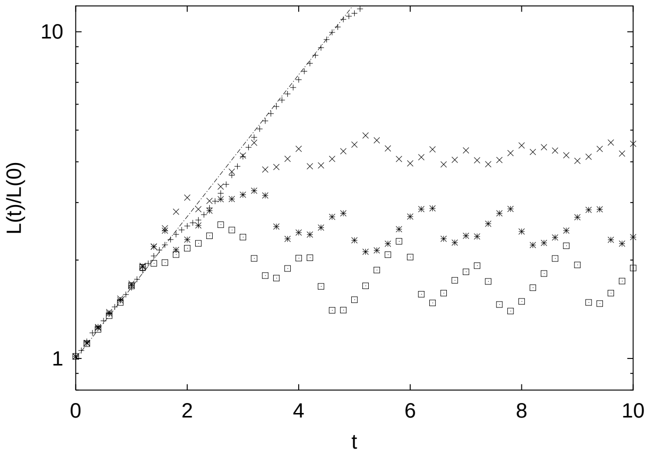

Figure 14: $\mathcal{L}(t)/\mathcal{L}(0)$ as a function of time for $U = 1.9$, $B = 1.1$ and $\omega = 1.1U$ for the passive $(+)$ and reactive case: from top $v_0 = 0.3\ (\times)$, $0.5\ (*)$, $0.7\ (\square)$. The straight line indicates the curve $\exp(\Lambda(1)t)$ with $\Lambda(1) \approx 0.5$, which has been directly measured.

originally at distance ℓ_0) become closer and closer, roughly as $\sim \ell_0 \exp(-\Lambda(1)t)$. When such a distance becomes of the order of $v_0 t$ the merging takes place, hence to leading order

$$t^* \propto \frac{1}{\Lambda(1)} \ln\left(\frac{\Lambda(1)\ell_o}{v_0}\right) . \tag{63}$$

In the asymptotic state ($t > t^*$) both the spatial and temporal structures of the flow become periodic.

Let us now switch to the effects of Lagrangian chaos on the asymptotic dynamics of front propagation. An immediate consequence of Eq. (63) is that the asymptotic front length (61) behaves as $L_{\rm f} \sim v_0^{-1}$ for values of v_0 small enough. Indeed,

$$L_{\rm f} \sim L e^{\Lambda(1)t^*} \sim \frac{L^2\Lambda(1)}{v_0} , \tag{64}$$

which is in fairly good agreement with the simulations [50]

It is worth remarking that even if the scaling (64) holds when chaos is present, in general it is not peculiar of chaotic flows. For instance, for the shear flow ($u_x = U\sin(y)$, $u_y = 0$) one has $v_{\rm f} = U + v_0$. On the other hand, since $v_{\rm f} \sim L_{\rm f} v_0$ [9], even if the shear flow is not chaotic $L_{\rm f} \sim 1/v_0$ for $U/v_0 \gg 1$. From the previous discussion, it seems that the front length dependence on v_0 is not an unambiguous effect of chaos on the asymptotic dynamics. But, looking at Fig. 13 it is apparent the spatial "complexity" of the front in the presence of Lagrangian chaos.

Let us now introduce an indicator to quantitatively evaluate this qualitative observation. Let us call $W_{\rm f}$ the size of the region in which burnt and unburnt material coexist. Introducing a measure, $\mu(x)$, in that region we can defined $W_{\rm f}$

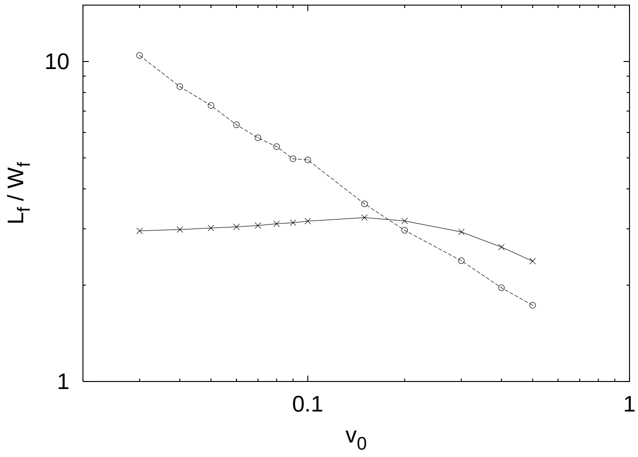

Figure 15: $L_{\rm f}/W_{\rm f}$ as a function of v_0 for the time dependent ($\circ$) and independent ($\times$) cases with parameters $U = 1.9$, $B = 1.1$, $\omega = 1.1U$ and the time independent case ($\times$) with $U = 1.9$..

as the standard deviation of $\mu(x)$ [50]:

$$\mu(x) = \frac{|\partial_x \tilde{\theta}(x)|}{\int \mathrm{d}x |\partial_x \tilde{\theta}(x)|}\,, \tag{65}$$

where $\tilde{\theta}(x) = 1/L \int_0^L \theta(x,y)\mathrm{d}y$, i.e.,

$$W_{\rm f} = \left(\int x^2 \mu(x) \mathrm{d}x - (\int x\mu(x)\mathrm{d}x)^2 \right)^{1/2}\,. \tag{66}$$

For a simple shear flow $W_{\rm f}$ and $L_{\rm f}$ display the same kind of dependence on v_0 (actually they are proportional). In generic chaotic flows there is an increasing of the front length, while chaotic mixing induces a decrease of $W_{\rm f}$. This is indeed what one observes in Fig. 15, where we show the ratio $L_{\rm f}/W_{\rm f}$ both for the non-chaotic and the chaotic flow. For the latter this ratio diverges for very small v_0 values as a signature of chaos. From a physical point of view the ratio $L_{\rm f}/W_{\rm f}$ is an indicator of the spatial complexity of the front. Indeed it indicates the degree of wrinkling of the front with respect to the size of the region in which the front is present. Loosely speaking, we can say that the *temporal* complexity of Lagrangian trajectories converts in the *spatial* complexity of the front.

Acknowledgments

We thank M. Abel, G. Boffetta, P. Castiglione, A. Celani, G. Lacorata, C. Lopez, R. Mancinelli, P. Muratore-Ginanneschi, A. Mazzino, R.A. Pasmanter, A. Torcini, M. Vergassola and E. Zambianchi for fruitful collaborations and interesting discussions during the last years.

References

[1] H.K. Moffatt, *Rep. Prog. Phys.*, **46**, 621 (1983).

[2] J.P. Bouchaud and A. Georges, *Phys. Rep.*, **195**, 127 (1990).

[3] G. Falkovich, K. Gawędzki, and M. Vergassola, Rev. Mod. Phys. **73**, 913 (2001).

[4] A. Crisanti, M. Falcioni, G. Paladin and A. Vulpiani, *La Rivista del Nuovo Cimento*, **14**, n.12, 1 (1991).

[5] L. Biferale, A. Crisanti, M. Vergassola and A. Vulpiani, *Phys. Fluids*, **7**, 2725 (1995).

[6] A. J. Majda, and P. R. Kramer, Phys. Rep. **314**, 237 (1999).

[7] V. Artale, G. Boffetta, A. Celani , M. Cencini and A. Vulpiani, *Phys. Fluids.* **9**, 3162 (1997).

[8] J. Xin, SIAM Review **42**, 161 (2000).

[9] N. Peters, *Turbulent combustion* (Cambridge University Press, 2000).

[10] A. N. Kolmogorov, I. G. Petrovskii, and N. S. Piskunov, Moscow Univ. Bull. Math. **1**, 1 (1937).

[11] R. A. Fisher, Ann. Eugenics **7**, 355 (1937).

[12] E. R. Abraham, Nature **391**, 577 (1998).

[13] J. Ross, S. C. Müller, and C. Vidal, Science **240**, 460 (1988).

[14] M. Abel, A. Celani, D. Vergni and A. Vulpiani, Phys. Rev. E **64**, 046307 (2001).

[15] P. Constantin, A. Kiselev, A. Oberman and L. Ryzhik, Arch. Rational Mechanics **154**, 53 (2000).

[16] B. Audoly, H. Beresytcki and Y. Pomeau, C. R. Acad. Sci. **328**, Série II b, 255 (2000).

[17] P. Constantin, A. Kiselev, L. Ryzhik, "Quenching of flames by fluid advection", arXiv.org e-Print archive nlin.CD/0006024

[18] A. R. Kerstein, W.T. Ashurst, F. A. Williams, Phys. Rev. A **37**, 2728 (1988).

[19] U. Frisch, A. Mazzino, and M. Vergassola, *Phys. Rev. Lett.*, **80**, 5532 (1998).

[20] G.I. Taylor, *Proc. Lond. Math. Soc. Ser. 2*, **20**, 196 (1921).

[21] E. Montroll and M. Schlesinger, in *Studies in Statistical Mechanics*, edited by E.W. Montroll and J.L.lebowitz vol. 11, p.1, North-Holland, Amsterdam, 1984.

[22] M.F. Schlesinger, B. West and J. Klafter, *Phys. Rev. Lett.*, **58**, 1100 (1987).

[23] M. Avellaneda and A. Majda, *Commun. Math. Phys.*, **138**, 339 (1991).

[24] M. Avellaneda and M. Vergassola, *Phys. Rev. E*, **52**, 3249 (1995).

[25] G. Matheron and G. De Marsily, *Water Resouces Res.*, **16**, 901 (1980).

[26] G.I. Taylor, *Proc. R. Soc. A*, **219**, 186 (1953);
Proc. R. Soc. A, **225**, 473 (1954).

[27] P. Castiglione, A. Mazzino, P. Muratore-Ginanneschi, A. Vulpiani, Physica D, **134**, 75 (1999).

[28] M.E. Fisher, J. Chem. Phys. **44**, 616 (1966).

[29] J.-P. Bouchaud, A. Georges, J. Koplik, A. Provat and S. Redner, *Phys. Rev. Lett.*, **64**, 2503 (1990).

[30] R. Mancinelli, D. Vergni and A. Vulpiani, Eur. Phys. Lett. **60**, 532 (2002);
R. Mancinelli, D. Vergni and A. Vulpiani, Physica D (2003), to appear.

[31] G.M. Zaslavsky, D. Stevens, and H. Weitzener, *Phys. Rev. E*, **48**, 1683 (1993).

[32] T.H. Solomon and J.P. Gollub, *Phys. Rev. A*, **38**, 6280 (1988).

[33] A.J. Lichtenberg and M.A. Lieberman *Physica D* **3**3, 211 (1988).

[34] Y.H. Ichikawa, T. Kamimura and T. Hatori *Physica D*, **2**9, 247 (1987).

[35] P. Leboeuf, *Physica D*, **1**16, 8 (1998).

[36] W.J. Cocke, *Phys. Fluids* **12**, 2488 (1969).

[37] U. Frisch, *Turbulence*, (Cambridge University Press, GB, 1995).

[38] G.Boffetta, M. Cencini, M. Falcioni and A. Vulpiani, Phys. Rep. **356**, 367 (2002).

[39] G. Boffetta, A. Celani, M. Cencini, G. Lacorata and A. Vulpiani Chaos **10**, 50 (2000).

[40] G. Lacorata, E. Aurell and A. Vulpiani, Ann. Geophys. **19**, 121 (2001).

[41] M.-C. Jullien, Phys. Fluids **15**, 2228 (2003).

[42] G. Boffetta, M. Cencini, S. Espa and G. Querzoli, Europhys. Lett. **48**, 629 (1999); Phys. Fluids **12**, 3160 (2000).

[43] G. Querzoli, Atmos. Env. **16**, 2821 (1996).

[44] L. F. Richardson, Proc. Roy. Soc. **A110**, 709 (1926).

[45] G. Boffetta, A. Celani, A. Crisanti and A. Vulpiani, Europhy. Lett., **46**, 177 (1999).

[46] G. Boffetta and A. Celani, Physica A **280**, 1 (2000).

[47] G. Boffetta and I. M. Sokolov, Phys. Rev. Lett. **88**, 094501 (2002).

[48] M. Freidlin, *Functional integration and partial differential equations* (Princeton University Press, Princeton NJ, 1985).

[49] P. F. Embid, A. J. Majda and P. E. Souganidis, Phys. Fluids **7** (8), 2052 (1995).

[50] M. Cencini, A. Torcini, D. Vergni, and A. Vulpiani, Phys. Fluids **15**, 679 (2003).

[51] W.T. Ashurst and G. I. Shivanshinsky, Comb. Sci. Tech. **80**, 159 (1991).

[52] P. D. Ronney, in *Modeling in Combustion Science*, pp. 3-22, Eds. J. Buckmaster and T. Takeno (Springer-Verlag Lecture Notes in Physics, 1994).

[53] B. Khouider, A. Bourlioux and A.J. Majda, Comb. Th. Model. **5** 295 (2001).

[54] V. Yakhot, Comb. Sci. Tech. **60**, 191 (1988).

[55] R. C. Aldredge, in *Modeling in Combustion Science*, pp. 23-35, Eds., J. Buckmaster and T. Takeno (Springer-Verlag Lecture Notes in Physics, 1994).

[56] R. C. Aldredge, Comb. and Flame **106**, 29 (1996).

[57] A. Oberman, PhD Thesis Univ. of Chicago 2001.

[58] A.K. Pattanayak, Physica D **148**, 1 (2001).

[59] A. Okubo and S.A. Levin, *Diffusion and ecological problems*, (Springer, New York, 2001).